Pak. J. Bot., 58(2) February, 2026.

ARTICLE | DOI: http://dx.doi.org/10.30848/PJB2026-2(21)

INVESTIGATION OF THE IMPACT OF [1-(2-ETHYL, 6-HEPTYL) PHENOL] ON MORPHOLOGICAL CHARACTERISTICS AND ULTRASTRUCTURES OF *ASPERGILLUS FUMIGATUS* AND *CANDIDA ALBICANS*

AMAL A.I. MEHKAWY [1], ABDULMOHSEN HUSSEN ALQHTANI[2], AHMED ALI[3], EMAN E HELAL[4] AND MOHAMMED YOSRI*[1]

[1]The Regional Center for Mycology and Biotechnology, Al-Azhar University, 11787, Nasr City, Cairo, Egypt
[2]Animal Production Department, Food and Agriculture Sciences College, King Saud University, Riyadh, Saudi Arabia
[3]Department of Animal and Veterinary Sciences, Clemson University, 29630, Clemson, South Carolina, United States of America
[4]International Islamic Center for Population Studies and Research, Al-Azhar University, Al-Darrassa ward 11651, Cairo, Egypt

*Corresponding author's email: mohammed.yosri@yhaoo.com

Abstract

Antimicrobial medications can be found in abundance in naturally occurring substances. Microbial resistance is the primary cause of the current global difficulty in accelerating the discovery of new antimicrobial medications. 1-(2-Ethyl, 6-Heptyl) Phenol (EHP) is a naturally occurring substance compound that was previously obtained by benzene from *Cuminum cyminum* (*C. cyminum,* cumin) Egyptian seeds. It demonstrated great action towards numerous pathogenic microorganisms. The study was done on how EHP affected the structural characteristics and ultrastructure of *Candida albicans* (*C. albicans*) and *Aspergillus fumigatus* (*A. fumigatus)*. Major modifications of morphological characteristics and alteration of ultrastructure of examined microbes were observed. Thus, this article describes the morphological and ultrastructural reductions in cellular structures that indicate the role of the evaluated natural product's antimicrobial efficacy which is derived from *Cuminum cyminum* which is cultivated in various regions.

Key words: *Cuminum cyminum; Aspergillus fumigatus; Candida albicans;* Morphology; Transmission electron microscope; Scanning electron microscope

Introduction

Plant extracts have been extensively studied for their antifungal, antibacterial, anticancer, and antiviral properties because they are low in toxicity and do not cause any adverse effects. Foods have been enhancing their flavor and scent for thousands of years through the use of herbs and spices (Bec *et al*., 2024; Jabeen *et al*., 2024; Önder *et al*., 2024). In addition to their culinary uses, ancient cultures understood the therapeutic benefits of utilizing spices and herbs. The antimicrobial capabilities of several herbal remedies, spices, and their constituent parts have been demonstrated by scientific investigations since the 19th century (Newman & Cragg, 2012; Sharifi *et al*., 2021; Khan *et al*., 2024).

Cuminum cyminum seeds possess hypoglycemic, carminative, stimulant, and antispasmodic properties. They are also used to cure burns, ulcers, and slow-acting fevers (Srinivasan, 2018; Norouzkhani *et al*., 2022; Strothmann *et al*., 2022). In addition to being antimalarial and helpful in dyspepsia and hoarseness, it may also treat colic and flatulence (Alomar *et al*., 2022; Mandal *et al*., 2023; Hamidian *et al*., 2023). It is still a traditional herbal cure in the East but is now mostly utilized in veterinary care in the West as a carminative. According to (Dini *et al*., 2022), it is meant to boost lactation and lessen pregnancy sickness. Another natural method of increasing breast size that shows potential is cumin. It reduces testicular or breast edema when applied as a poultice (Goodarzi *et al*., 2020; Alqethami & Aldhebiani, 2021; Buathong & Duangsrisai, 2023).

The EHP compound was extracted from *C. cyminum* (cumin) seeds using benzene, and it demonstrated remarkable potency as an antifungal agent (Mekawey *et al*., 2009). EHP molecule demonstrated antibacterial, antiviral, and anticancer properties in vitro as well (Mekawey & El-Metwally, 2019).

Fungal infections pose more challenging therapeutic issues, particularly for hospitalized patients, where prolonged antibiotic use kills both pathogenic and beneficial bacteria, changing the balance of microorganisms in the various body areas and leading to fungal overgrowth (Younis *et al*., 2019). The present work examined the effects of a 1-(2-Ethyl, 6-Heptyl) Phenol molecule on the morphological characteristics and ultrastructure of eukaryotic cells, including fungal cells. Specifically, filamentous fungi such as *A. fumigatus* and unicellular fungi such as *C. albican* were studied.

Material and Methods

Tested substance: The following formula structure of the EHP compound was used; it's obtained by Mekawey *et al*., (2009).

The tested microbial isolates *A. fumigatus* (ATCC96918) and *C. albicans* (ATCC10231*)* were obtained from the Regional Center for Mycology and Biotechnology (RCMB), Al-Azhar University, Cairo, Egypt.

Antimicrobial action and minimal inhibitory concentration (MIC).

Received: 15-12-2024 | Revised: 06-08-2025 | Accepted: 16-08-2025 | Online: 02-12-2025

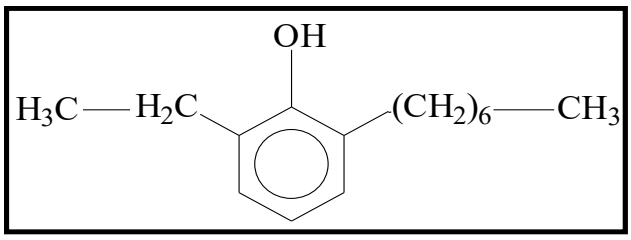

[1-(2-Ethyl, 6-Heptyl) Phenol] (EHP)

The agar diffusion method was used. In brief, Petri plates (150 × 20 mm –Therrmo Scientific, USA) were filled with 40 ml of hardened malt followed by spreading of the suspension of fungus and yeast, respectively. The holes in the plates were created with a 1 cm cork borer. 100 µl of EHP, which had been dispersed in 5% dimethyl sulfoxide (DMSO) (Sigma-Aldrich), was then added to each well to a final level of 10 mg/ml. A 5% DMSO was added to as a negative control well. Standard drugs were applied. The plates were left at 37.0 ± 2°C for yeast at 28 ± 2°C for fungi for 24 to 48 hours. Three sets of assays were performed (Younis *et al*., 2019; Huo *et al*., 2021).

Seven concentrations were created by serially diluting 1 mg/ml of each EHP dissolved in 5% DMSO (1:2) with culture broth media containing 5% DMSO: 1, 0.5, 0.25, 0.125, 0.0625, 0.0312, and 0.0156 mg/ml. After that, 96-well plates (Thermo fisher Scientific, USA) were filled with 200 µl of each EHP dilution or the negative control (5% DMSO without extract), and 10 µl of microbial suspension was inserted into every well for inoculation. At 410 nm, absorbance was detected (Younis *et al*., 2019).

Microscopic examination

Classical imaging: An Image analyzer microscope was applied for light microscopic investigation. Soft imaging system GmbH software (analysis ® pro ver. 3.0 model 1999 at the Regional Center for Mycology and Biotechnology, AL-Azhar University, was applied to test the alteration of morphological characteristics of test fungal isolates. The magnification power (X 400) was applied for *A. fumigatus* after 48 hours of incubation and also used for *C. albicans* after 24 hours of incubation time, using either phase-contrast or bright field optics. Three plates were obtained from every isolate, and at least 20 tiny areas were investigated. Close inspection of cultures, paying special attention to conidiophore, vesicle, stigmata, and conidiophore for *A. fumigatus* was done and measurements were taken, while pseudo-mycelium, germ tubes, bud cells, and normal cells for *C. albicans* were made and measured from materials mounted in methylene blue stain (Zhang *et al*., 2022).

Scanning electron microscope: Blocks of the tested microbial isolate under investigation were prepared at the National Research Centre in Dokki, Cairo, Egypt, and subjected to SEM examination. Through applying (The LEICA EM AP tissue processor model (A-1170), fixation and dehydration processes were carried out. Squares of agar measuring six to eight millimeters that had fungal growth were removed from the cultures. After that, the squares were fixed for 12 hours at 4°C by submerging them in 2% (w/v) aqueous osmium tetroxide (OsO_4). To get rid of extra OsO_4, the fixing agent was left to reach ambient temperature and then cleaned three times, for ten minutes each, in distilled water. Materials that had been fixed and cleaned were immersed and dried using an ethanol series that was graded in 10% increments, going from 10% to 90%, and then absolute ethanol. Using a pressure bomb, dehydrated samples were critical point dried. After that, 0.9 mm copper stubs were joined to the critical point-dried specimens by a carbon glue. Samples were coated with gold (about 50 nm thick) by Polar Instruments Inc., Doylestown, PA, and subsequently analyzed using a JEOL JSM-35LV Scanning Electron Microscope in the high-vacuum mode (Chow *et al*., 2019; Alizadeh *et al*., 2021).

Transmission electron microscope: One-millimeter blocks of investigated isolates, one treated with EHP compound, were implanted in 2% agar, immersed in 3% glutaraldehyde – 1% paraformaldehyde at 5ºC for an hour, and dehydrated using a graded series of ethanol. Living cells were placed between two copper discs for quick freezing and freeze-substitution. Next, acetone was used to freeze-substitute the cells, which contained 2.0% osmium tetroxide at -80°C for two days. Cells were preserved at room temperature in a 0.1 M phosphate buffer (pH 7.3) containing 3% glutaraldehyde and 1% paraformaldehyde for 30 to 60 minutes or at 4ºC for an entire night in order to perform freeze replacement following glutaraldehyde fixation. Centrifugation is used to gather the cells, and they are then quickly frozen using propane and freeze-replaced in acetone with 2% osmium tetroxide for two days at 80ºC. Following their various fixes and dehydrations, these samples were implanted in epoxy resin and polymerized for 24 hours at 60°C. Using a knife and an ultramicrotome (Leica Germany), ultrathin slices were sliced to a thickness of 70–90 nm and placed on copper grids. They undergo staining with uranyl acetate and lead citrate and are examined in the National Research Center's JEM 12000EX TEM (JEOL, Japan) at 80 kv (Sayed *et al*., 2022).

Statistical analysis

All experiments were done three times. The output was written as means ±standard deviation (SD), and the student T-test was applied to determine the differences, where $p \leq 0.05$ considered as significant difference.

Results

Antimicrobial action and MIC of EHP towards tested microbes EHP showed a promising inhibition zone towards *A. fumigatus* (ATCC96918) which was 17.9 ± 1.80 mm with MIC= 125.0 ± 0.6 µg/ml. Furthermore, EHP has a notable impact on *C. albicans* (ATCC10231) with an inhibition zone of 18.8 ± 1.5 mm with MIC= 62.5 ± 0.1 µg/ml (Table 1).

Table 1. Antimicrobial role and MIC of EHP versus *A. fumigatus* and *C. albicans*.

Tested microorganisms	Inhibition zone (mm) of EHP compound	Inhibition zone (mm) Amphotericin B	MIC of EHP compound(µg/ml)	MIC of Amphotericin B (µg/ml)
A. fumigatus (ATCC96918)	17.9 ± 1.80	22.7 ± 0.6	125.0 ± 0.6	1.85 ± 0.2
C. albicans (ATCC10231)	18.8 ± 1.5	24.4 ± 1.1	62.5 ± 0.1	1.1 ± 0.1

Table 2. Image Analyzer measurements of *Aspergillus fumigatus* affected by EHP.

Fungal structure	Control (without any effect)	Using MIC of EHP compound	Comment
	Mean of diameters (µm)		
Mycelium	6.5 ± 0.1	4.2 ± 0.2	
Conidiophores	5.3 ± 0.2	3.0 ± 0.1	- Chlamydospores formed; Conidial stage absents
Vesicle	18.2 ± 0.1	8.9 ± 0.3	
Sterigmata	4.8 ± 0.1 x 2.4 ± 0.2	2.8±0.3 x 3.5 ± 0.1	- Great reduction in all morphological features
Conidia	3.0 ± 0.3	1.5 ± 0.1	

Table 3. Scanning electron measurements of *Aspergillus fumigatus* affected by EHP.

Fungal structure	Control (without any effect)	Using MIC of EHP compound	Comment
	Mean of diameters (µm)		
Conidiophores	40.0 ± 0.4	20.0 ± 0.6	Great reduction in all morphological features
Conidia	15.2 ± 0.3	7.2 ± 0.2	

Table 4. Image analyzer measurements of *C. albicans* affected by EHP.

Fungal structure	Control (without any effect)	Using MIC of EHP compound	Comment
	Mean of diameters (µm)		
Pseudomycelium	2.2 ± 0.2	4.2 ± 0.1	- Elongation of many of yeast cells
Yeast cells	4.2 ± 0.1 x 2.1 ± 0.2	6.7 ± 0.1 x 3.8 ± 0.2	- Great reduction in number of yeast cells
Germ tube	20.1 ± 0.1 x 2.0 ± 0.3	10.6 ± 0.2 x 1.0 ± 0.3	

Table 5. Scanning electron measurements of *C. albicans* affected by EHP.

Fungal structure	Control (without any effect)	Using MIC of EHP compound	Comment
	Mean of diameters (µm)		
Pseudomycelium	2.5 ± 0.1	5.0±0.2	- Elongation of many of yeast cells
Yeast cells	4.7 ± 0.2 x 2.5 ± 0.1	7.2 ± 0.2 x 4.3 ± 0.3	- Great reduction in number of yeast cells
Germ tube	25.0 ± 0.3 x 2.4 ± 0.1	12.0 ± 0.2 x 1.1 ± 0.2	

The results of the image analyzer revealed that a significant reduction ($p \leq 0.05$) in the size of morphological features of the tested fungus after treatment with 125 µg/ml of EHP (Fig. 1, Table 2) occurred; the mycelia and conidiophores both dramatically decreased in their diameter by 2.3 µm. The vesicle became smaller in its size by 9.3 µm as compared with the control. Great distortion was occurred in the sterigmata and they became shorter by 2.0 µm and swollen by 1.1 µm, while the conidia decreased in diameter by 1.5 µm. In addition, very big chlamydospores were obtained. The microorganism managed to maintain its aspergillate shape, but with every morphological characteristic changed (Table 2). However, conidiophores decreased in diameter by 2.7 µm, and vesicles reduced by 11.3 µm. Sterigmata were reduced by 1.7 µm and swollen by 1.5 µm, whereas different distorted sterigmata forms were seen: increased, confined, and lessened. Also, a significant reduction in size of conidia and conidiophores ($p \leq 0.05$) upon treatment using 125 µg/ml of EHP, where conidia became smaller by 1.3 µm. These results were mostly in accordance with those of the image analyzer results. Comparable scanning electron microscope images highlight the essential role of EHP towards *A. fumigatus* especially against the reduction of conidiophores and conidial dimensions (Fig. 2, Table 3).

Besides, many modifications to the cellular structure of *C. albicans* treated by 62.5 µg/ml of EHP using an image analyzer might be summed up as the gathering of *C. albicans* cells and there was a great reduction of their sizes, while many distortions were obtained in many *C. albicans* cells, like elongation and swelling when treated with EHP. Besides, their number decreased and the pseudo-mycelium disappeared (Fig. 3 & Table 4).

SEM results show the remarkable changes in the morphological structure of conidia and pseudomycelium of *C. albicans* grown in the presence of EHP compound. Most of the yeast cells were greatly reduced in size, but some cells became elongated and swollen (Fig. 4 and Table 5).

In the present study, the action of EHP significantly reduced ($p \leq 0.05$) the cellular organelles of *A. fumigatus* and *C. albicans* upon investigation using TEM microscopy. The present study showed that several changes and distortions of sub-organelles of *A. fumigatus* were obtained upon using MIC of EHP. In general, cell wall and cell membrane were reduced in thickness; in contrast, great reductions in mitochondria and nucleus diameters were observed (Table 6). Besides, (Fig. 5) showed that all fungus parts appeared inside semi-empty, and all sub-organs were distorted in their shape; separation and shrinking of the cell membrane away from the cell wall was observed. Oil drops appeared and pigment was precipitated around the cell membrane. The number of vacuoles decreased, while a very large vacuole was seen. Finally, a thick sheath appeared around the conidia.

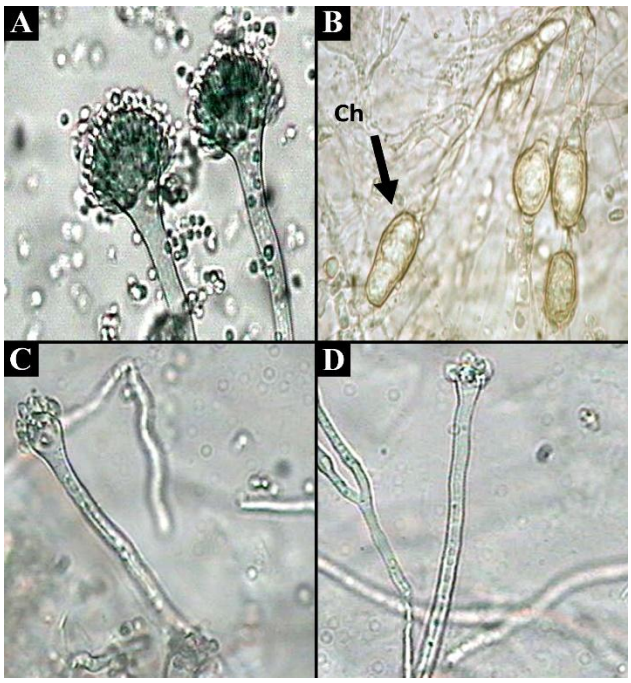

Fig. 1. Image analyzer examination of *Aspergillus fumigatus* at (X 400) A- *A. fumigatus* control; B-C-D *A. fumigatus* treated with EHP; Ch- chlamydospore.

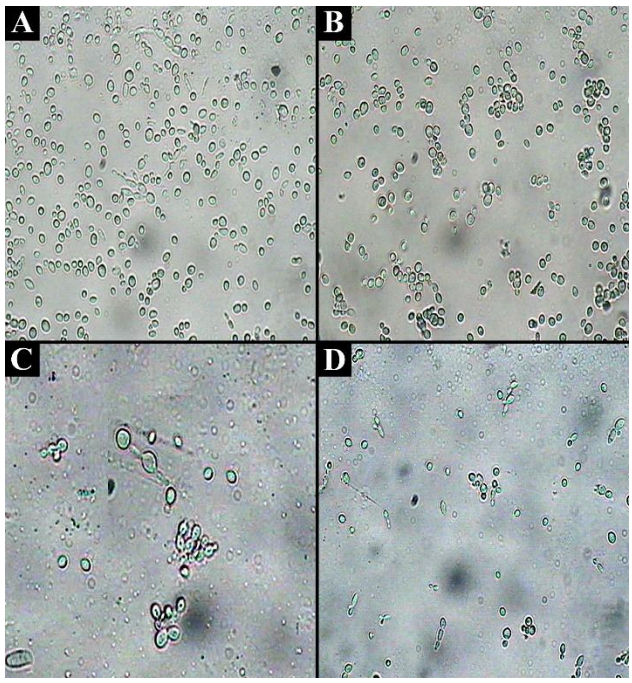

Fig. 3. Image analyzer examination of *C. albicans* at (X 400) A- *C. albicans* control; B-C- D *C. albicans* treated with EHP.

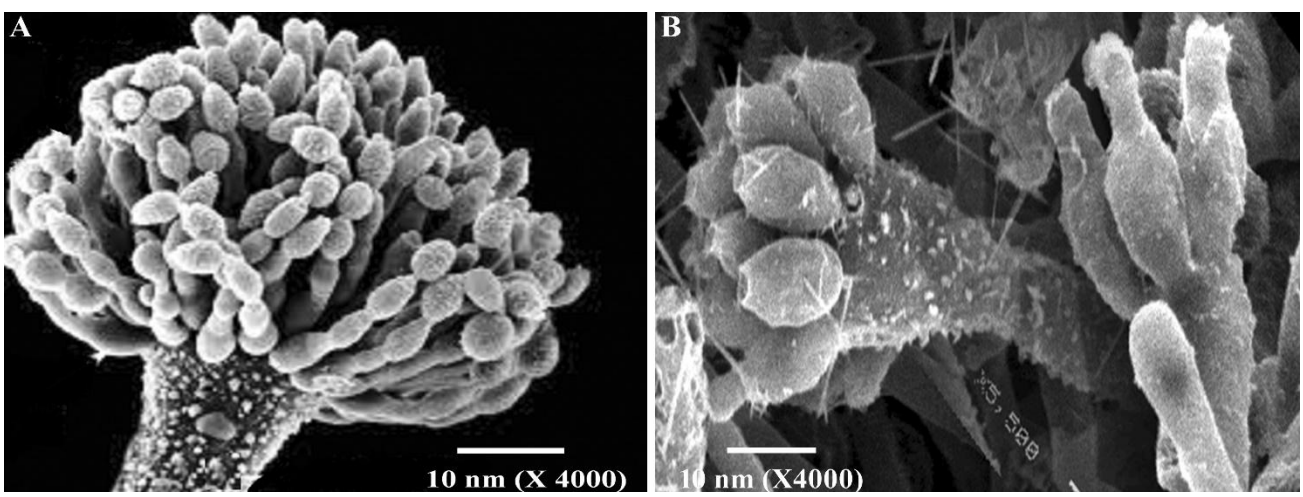

Fig. 2. Scanning electron microscope images of *A. fumigatus.* A- *A. fumigatus* control; B- *A. fumigatus* treated with EHP.

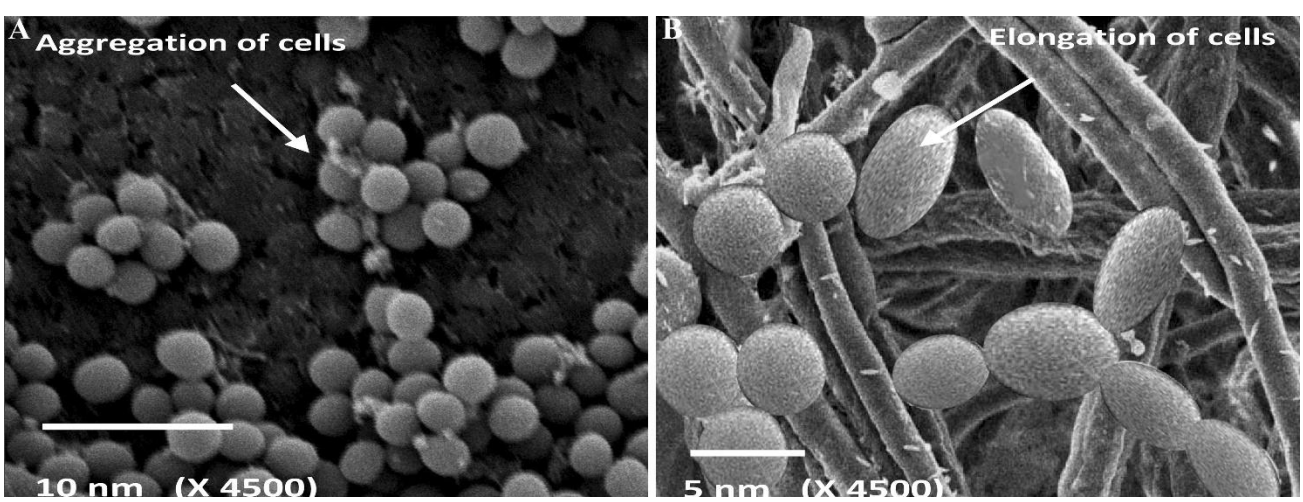

Fig. 4. Scanning electron micrographs of *C. albicans*. A- *C. albicans* control; B- *C. albicans* treated with EHP.

Table 6. Ultrastructure measurement of various structures of *A. fumigatus* affected by EHP.

Stress compound / Fungal ultra- structures	Control	EHP stress
	Mean of diameters (µm) at magnification (X 25000)	
Cell wall (CW)	210.1 ± 0.1	99.5 ± 1.1
Cell membrane (CM)	168.6 ± 1.1	64.3 ± 1.4
Mitochondria (L.S.) *	3519.0 ± 1.9 x 347.8 ± 1.8	514.3 ± 1.6 x 102.6 ± 1.4
Mitochondria (T.S.) *	429.5 ± 1.3 x 303.11.2	150.1 ± 1.5 x 88.2 ± 1.6
Nucleus (N)	2220.5 x 1160.2	760 x 576.7

* [(L.S): Longitudinal section; (T.S): Transverse section]

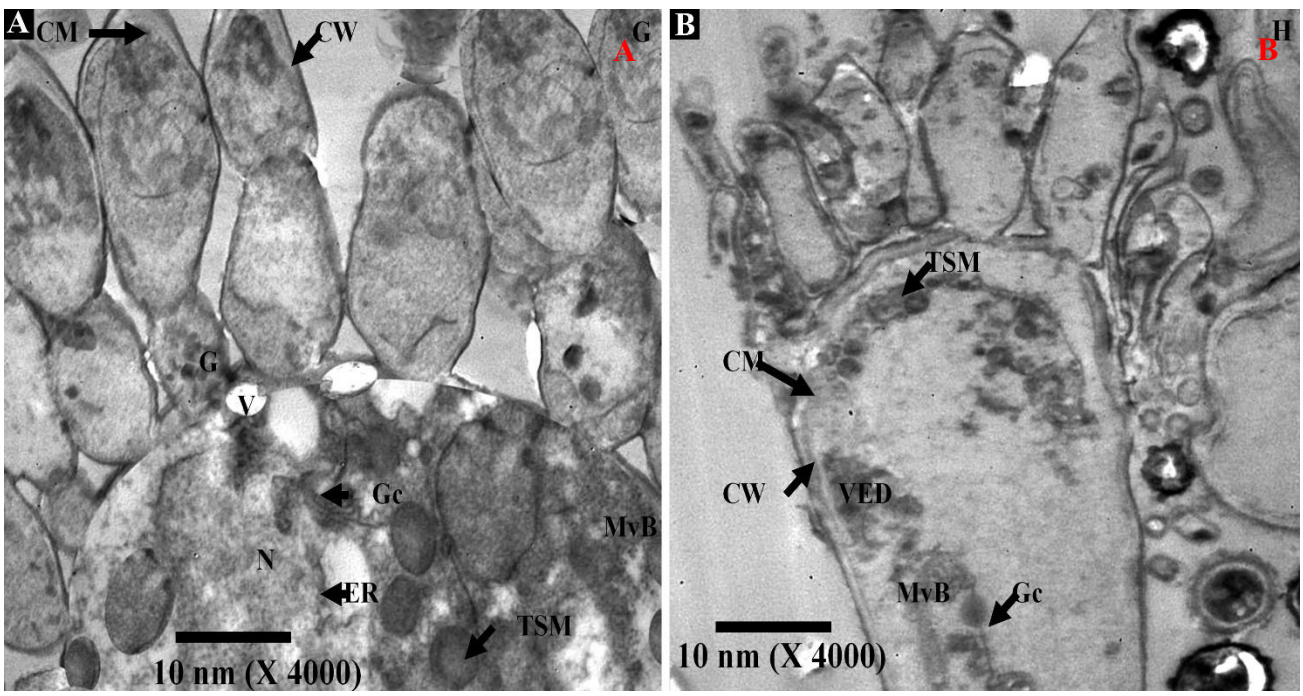

Fig. 5. Transmission electron micrographs of *Aspergillus fumigatus.* A- *A. fumigatus* control; B- *A. fumigatus* treated with EHP

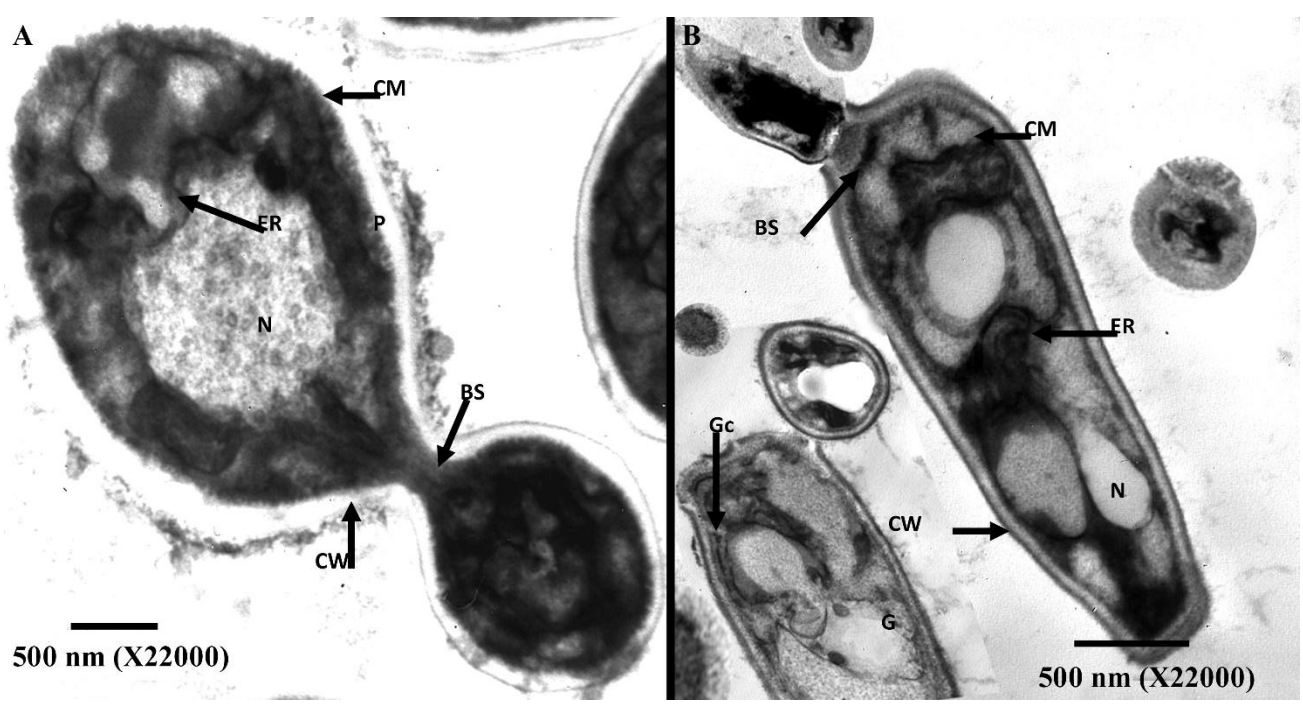

Fig. 6. Transmission electron micrographs of *Candida albicans* A- *C. albicans* control; B- *C. albicans* treated with EHP * Cell Wall (CW); Cell Membrane (CM); Transverse Section of Mitochondria (TSM); Nucleus (N); nucleolus (nu); Lipid Granule (LG); Vacuole (V); Multivesicular Bodies (MvB); Ribosomes (R); Golgi cisternae (Gc); Budding scare (BS); Endoplasmic Reticulum (ER); Plasmolysis (P); Vacuolated electron dense bodies (VED); Polysaccharide granules (G); Worrion bodies(WB); Septum (S) and Sheath (Sh).

Table 7. Ultrastructure measurements of *C. albicans* affected by EHP.

Fungal ultra-structures	Control	EHP stress
	Mean of diameters (µm)	
Cell wall (CW)	269.5 ± 0.1	150.8 ± 0.3
Cell membrane (CM)	55.3 ± 0.2	24.5 ± 0.4
Mitochondria (T.S.M)	284.7 ± 0.3 X 106.5 ± 0.5	124.8 ± 0.6 X 75.6 ± 0.2
Nucleus (N)	2385.9 ± 6.5 X 1180.7 ± 7.5	1230.2 ± 3.5 X680.5 ± 4.5

* Cell Wall (CW); Cell Membrane (CM); Transverse Section of Mitochondria (TSM); Longitudinal Section of Mitochondria (LSM); Nucleus (N); nucleolus (nu); Lipid Granule (LG); Vacuole (V); Multivesicular Bodies (MvB); Ribosomes (R); Golgi cisternae (Gc); Endoplasmic Reticulum (ER); Plasmolysis (P); Vacuolated electron dense bodies (VED); Polysaccharide granules (G); Worrion bodies (WB); Septum (S)

In the present study, *C. albicans* was affected by the EHP compound, where several changes occurred in its shape; unicellular cells became very tall and swollen in size, and the shape of the cell converted from oval to cylindrical (Fig. 6). Also, (Table 7) showed that the cell wall was reduced in diameter, while cell membrane, nucleus, and mitochondria diameters were reduced in their thickness.

Discussion

Natural substances are currently receiving significant attention as food additives because of their security, ease of use, and accessibility – especially those derived from edible and therapeutic plants. Among these is cumin (*Cuminum cyminum*), a plant that belongs to the Apiaceae family. Saudi Arabia, China, India, and the nations that border the Mediterranean Sea are the principal places where it is grown (Ramadan *et al*., 2012; Mohammadpour *et al*., 2012). Popular fragrant herbs and edible spices include cumin seeds. It is mostly utilized in conventional and veterinary medicine as a stimulating agent (Roche *et al*., 2016; Sharma *et al*., 2016). Cumin is a strong contender to be employed as a protective agent against different microorganisms because of all these qualities (Rebey *et al*., 2017).

Using antimicrobial drugs has sparked an uprising of research into novel instruments and approaches that might enhance, automate, and speed up more targeted and morphological changes (Dauwalder *et al*., 2016; Zhang *et al*., 2017; Hart *et al*., 2019). When examining the surface structure of biological materials, scanning electron microscopy (SEM) is widely utilized. New, potent antifungal medicines are required for *A. fumigatus* and *C. albicans*, which are becoming more and more dangerous to humans and animals. Numerous morphological techniques are being employed for antifungal testing, with transmission electron microscopy (TEM) being one of the most popular ones (Salazar & Arranz-Trullen, 2019; Grigor'eva *et al*., 2020; Sherif *et al*., 2023). In this study TEM and SEM were employed in order to examine the microscopic alterations in *A. fumigatus* and *C. albicans* by 1-(2-Ethyl, 6-Heptyl) Phenol extracted from *C. cyminum*.

The most prevalent class of natural products found in plants is phenolic compounds, which exhibit a variety of biological characteristics, such as antioxidant and antifungal activities (Simonetti *et al*., 2020; Panzella *et al*., 2020; Yusoff *et al*., 2022). There aren't numerous investigations on the antifungal properties of plant extracts, and none that highlight the function of 1-(2-Ethyl, 6-Heptyl) Phenol. Similarly, the fact that cumin seeds have long been used to cure a wide variety of ailments is evidence of their exceptional bioactive potential. Therefore, cumin bioactive molecules may represent a potential source of novel antioxidant and anti-inflammatory phenolic compounds that are safer than those found in current medications (Agregan *et al*., 2021; Brahmi *et al*., 2022).

This study illustrated the antimicrobial effect of MIC of 1-(2-Ethyl, 6-Heptyl) Phenol on suppression of *C. albicans* and *A. fumigatus* cells through significant reduction of different structures, especially the cell walls, nucleus, and mitochondria. The fungal cell wall is an active structure that permits interaction with the outside world and other organisms while shielding fungal cells from osmotic pressure fluctuations and other adverse environmental conditions. In addition to keeping the shape and integrity of the cell during stressful circumstances, the cell wall functions as a signaling hub for fungal cells (Gow *et al*., 2017; Lima *et al*., 2019). It does this by mediating interactions with the outside world through receptors that set off an intricate chain reaction of signals inside the cell. The cell wall is an appropriate target for the investigation of novel antifungal drugs because of its unique structure and architectural organization, crucial functional role, and lack of its main constituents in mammalian cells (Garcia-Rubio *et al*., 2020). It could be seen that 1-(2-Ethyl, 6-Heptyl) Phenol significantly reduces the dimension of the cell wall in both *C. albicans* and *A. fumigatus*.

The mitochondria have a variety of functions in eukaryotic cell physiology, including fungi and yeast, which drives a variety of disease-related processes, including pathogen fitness, developmental and morphogenetic changes, and resistance to antifungal drugs (Fenton *et al*., 2021; Fernandes *et al*., 2024). 1-(2-Ethyl, 6-Heptyl) Phenol led to a dramatic shrink of mitochondria dimensions. The nuclei play a traditional function in inheritance and store phosphorus and nitrogen in the structure of DNA (Faoro *et al*., 2022). The tested molecule led to a notable reduction in the dimensions of nuclei.

Conclusions

[1-(2-Ethyl, 6-Heptyl) Phenol] extracted from *Cuminum cyminum* could be used to combat both *Aspergillus fumigatus* and *Candida albicans* upon structural alteration of various organelles examined by light, transmission and electron microscopes.

Acknowledgment

Non applicable

Funding

This work was supported by the Ongoing Research Funding Program, (ORF-2025-439), King Saud University, Riyadh, Saudi Arabia.

References

Agregan, R., P.E.S. Mankato, X. Feng, G. Astray, B. Gullon and J.M Lorenzo. 2021. Recent advances in the extraction of polyphenols from eggplant and their application in foods. *LWT*., 146: 111381.

Alizadeh, B., M. Noshad and F. Falah. 2019. Cumin essential oil: Phytochemical analysis, antimicrobial activity and investigation of its mechanism of action through scanning electron microscopy. *Microb. Pathog*., 136: 103716.

Alomar, H.A., N. Fathallah, M.M. Abdel-Aziz, T.A. Ibrahim and W.M. Elkady. 2022. GC-MS profiling, anti-helicobacter pylori, and anti-inflammatory activities of three apiaceous fruits' essential oils. *Plants* (*Basel*)., 11(19): 2617.

Alqethami, A. and A.Y. Aldhebiani. 2021. Medicinal plants used in Jeddah, Saudi Arabia: Phytochemical screening. *Saudi J. Biol. Sci*., 28(1): 805-812.

Bec, N., C. Larroque and C. Armijos. 2024. Exploring Southern Ecuador's Traditional Medicine: Biological screening of plant extracts and metabolites. *Plants* (*Basel*)., 13(10): 1422.

Brahmi, F., F. Blando, R. Sellami, S. Mehdi, L. de Bellis, C. Negro, H. Haddadi-Guemghar, K. Madani and L. Makhlouf-Boulekbache. 2022. Optimization of the conditions for ultrasound-assisted extraction of phenolic compounds from *Opuntia Ficus-Indica* [L.] Mill. flowers and comparison with conventional procedures. *Ind. Crops Prod*., 184: 114977.

Buathong, R. and S. Duangsrisai. 2023. Plant ingredients in Thai food: a well-rounded diet for natural bioactive associated with medicinal properties. *Peer J*., 11: e14568.

Chow, J., H.M. Dionne, A. Prabhakar, A. Mehrotra, J. Somboonthum, B. Gonzalez, M. Edgerton and P.J. Cullen. 2019. Aggregate filamentous growth responses in yeast. *mSphere*, 4(2): e00702-18.

Dauwalder, O., L. Landrieve, F. Laurent, M. de Montclos, F. Vandenesch and G. Lina. 2016. Does bacteriology laboratory automation reduce time to results and increase quality management? *Clin. Microbiol. Infect*., 22: 236-243.

Dini, S., Q. Chen, F. Fatemi and Y. Asri. 2022. Phytochemical and biological activities of some Iranian medicinal plants. *Pharm. Biol*., 60(1): 664-689.

Faoro, F., A. Faccio and R. Balestrini. 2022. Contributions of ultrastructural studies to the knowledge of filamentous fungi biology and fungi-plant interactions. *Front. Fungal Biol*., 2: 805739.

Fenton, A.R., T.A. Jongens and E.L.F. Holzbaur. 2021.Mitochondrial dynamics: Shaping and remodeling an organelle network. *Curr. Opin. Cell Biol*., 68: 28-36.

Fernandes, F.A.V., D.C. Arruda, G.N.P. Santana, L.V.G. Longo, M.C.M. Cesar, D.A. da Matta, O.S.M. Borba, R.C. Monteiro, M. de Moura Bello, L.H.B. de Moura, D.J. Neto, S. Yarak, P. de Camargo, O.F. Gompertz and M.M. Ogawa. 2024. Morphological and ultrastructural changes in fungal agents after LASER application. *Int. J. Dermatol*., 63(2): 217-223.

Garcia-Rubio, R., H.C. de Oliveira, J. Rivera and N. Trevijano-Contador. 2020. The fungal cell wall: Candida, Cryptococcus and *Aspergillus* species. *Front. Microbiol*., 10: 2993.

Goodarzi, S., M.J. Tabatabaei, J.R. Mohammad, F. Shemirani, S. Tavakoli, M. Mofasseri and Z. Tofighi. 2020. Cuminum cyminum fruits as source of luteolin- 7-O-glucoside, potent cytotoxic flavonoid against breast cancer cell lines. *Nat. Prod. Res*., 34(11): 1602-1606.

Gow, N.A.R., J.P. Latge and C.A. Munro. 2017. The fungal cell wall: Structure, biosynthesis, and function. *Microbiol. Spectr.*, 5: 267-292.

Grigor'eva, A., A. Bardasheva, N. Tupitsyna, N. Amirkhanov Tikunova, D. Pyshnyi, M. Kleshev and E. Ryabchikova. 2020. Changes in the Ultrastructure of *Candida albicans* Treated with Cationic Peptides**.** *Microorganisms*, 8(4): 582.

Hamidian, M., A. Salehi, R. Naghiha, M.M. Dehnavi, I. Castangia and M.N. Mirfathi. 2023. The comparative perspective of phytochemistry and biological properties of the Apiaceae family plants. *Sci. Rep.*, 13(1): 12390.

Hart, E. and M. Nguyen. 2019. A systematic review of the impact of antifungal stewardship interventions in the United States. *Ann. Clin. Microbiol. Antimicrob*., 18: 24.

Huo, Y.Y., T.T. Li, J. Yang, H.Y. Huang, C.J. Chen, F.R. Xu and X. Dong. 2021. Chemical constituents of the essential oil from *Cuminum cyminum* L. and Its antifungal activity against *Panax notoginseng* Pathogens. *Chem. Biodiv*., 18(12): e2100638.

Jabeen, T., M.S. Amjad, K. Ahmad, R.W. Bussmann, H. Qureshi and I. Vitasović-Kosić. 2024. Ethnomedicinal plants and herbal preparations used by rural communities in Tehsil Hajira (Poonch District of Azad Kashmir, Pakistan). *Plants* (*Basel*)., 13(10): 1379.

Khan, A., M. Ahmad, A. Sultan, R. Khan, J. Raza, S.Z. Ul Abidin, S. Khan, M. Zafar, M.N. Uddin and M. Kazi, 2024. Herbal Spices as Food and Medicine: Microscopic authentication of commercial herbal spices. *Plants* (*Basel*), 13(8): 1067.

Lima, S.L., A.L. Colombo and J.N. de Almeida. 2019. Fungal cell wall: emerging antifungals and drug resistance. *Front. Microbiol*., 10: 2573.

Mandal, D., T. Sarkar and R. Chakraborty. 2023. Critical review on nutritional, bioactive, and medicinal potential of spices and herbs and their application in food fortification and nanotechnology. *Appl. Biochem. Biotechnol*., 195(2): 1319-1513.

Mekawey, A.A., M.M. Mokhtar and R.M. Farrag. 2009. Antitumor and antibacterial activities of [1-(2-Ethyl, 6-Heptyl) Phenol] from *Cuminum cyminum* seeds. *J. Appl. Sci. Res*., 5(11): 1881-1888.

Mekawey, A.A. and M.M. El-Metwally. 2019. Impact of nanoencapsulated natural bioactive phenolic metabolites on chitosan nanoparticles as aflatoxins inhibitor. *J. Basic Microbiol*., 59(6): 599-608.

Mohammadpour, H., E. Moghimipour, I. Rasooli, M.H. Fakoor, A.S. Alipoor, M.S. Shehni and Z. Jalili. 2012. Chemical composition and antifungal activity of *Cuminum cyminum* L. essential oil from Alborz Mountain against *Aspergillus* species. Jundishapur *J. Nat. Pharm. Prod*., 7: 50-55.

Norouzkhani, N., A.G. Karimi, N. Badami, E. Jalalifar, B. Mahmoudv, A. Ansari, S.N. Pakrou, D. Alijanzadeh, S. Aghakhani, R. Shayestehmehr, M. Arzaghi, Z. Sheikh, Y. Salami, M.H. Marabi, A. Abdi and N. Deravi. 2022. From kitchen to clinic: Pharmacotherapeutic potential of common spices in Indian cooking in age-related neurological disorders. *Front. Pharm.*, 13: 960037.

Newman, D.J. and G.M. Cragg. 2012. Natural products as sources of new drugs over the 30 years from 1981 to 2010. *J. Nat. Prod*., 75: 311-335.

Önder, S., Ç.D. Periz, S. Ulusoy, S. Erbaş, D. Önder and M. Tonguç. 2024. Chemical composition and biological activities of essential oils of seven Cultivated Apiaceae species. *Sci Rep*., 14(1): 10052.

Panzella, L., F. Moccia, R. Nasti, S. Marzorati, Verotta, L. and A. Napolitano. 2020. Bioactive phenolic compounds from agri-food wastes: An update on green and sustainable extraction methodologies. *Front. Nutr*., 7: 60.

Ramadan, M.F., M.M.S. Asker and M. Tadros. 2012. Antiradical and antimicrobial properties of cold-pressed black cumin and cumin oils. *Eur. Food Res. Technol*., 234: 833-844.

Roche, J., A. Bouniols, M. Cerny, Z. Mouloungui and O. Merah. 2016. Fatty acid and phytosterol accumulation during seed ripening in three oilseed species. *Int. J. Food Sci. Technol*., 51: 1820-1826.

Rebey, I.B., S. Bourgou, F.Z. Rahali, K. Msaada, R. Ksouri and B. Marzouk. 2017. Relation between salt tolerance and biochemical changes in cumin (*Cuminum cyminum* L.) seeds. *J. Food Drug Anal.*, 25(2): 391-402.

Salazar, V.A. and J. Arranz-Trullen. 2019. Insight into the antifungal mechanism of action of human RNase N-terminus derived peptides. *Int. J. Mol. Sci*., 20: 558.

Sayed, R., N.A. Safwat, B.H. Amin and M. Yosri. 2022. Study of the dual biological impacts of aqueous extracts of normal and gamma-irradiated *Galleria mellonella* larvae. *J. Taibah. Univ. Med. Sci*., 17(5): 765-773.

Sharifi, A., A. Mohammadzadeh, T.Z. Salehi, P. Mahmoodi and A. Nourian. 2021. *Cuminum cyminum* L. Essential Oil: A promising antibacterial and antivirulence agent against multidrug-resistant *Staphylococcus aureus*. *Front. Microbiol*., 12: 667833.

Sharma, L.K., D. Agarwal, S.S. Rathore, S.K. Malhotra and S.N. Saxena. 2016. Effect of cryogenic grinding on volatile and fatty oil constituents of cumin (*Cuminum cyminum* L.) genotypes. *J. Food Sci. Technol*., 53: 2827-2834.

Sherif, M.M., H.H. Elshikh, M.M. Abdel-Aziz, M.M. Elaasser and M. Yosri. 2023. *In Vitro* Antibacterial and phytochemical screening of *hypericum perforatum* extract as potential antimicrobial agents against multi-drug-resistant (MDR) Strains of Clinical Origin. *Biomed. Res. Int*., 2023: 6934398.

Simonetti G., E. Brasili and G. Pasqua. 2020. Antifungal activity of phenolic and polyphenolic compounds from different matrices of *Vitis vinifera* L. against human pathogens. *Molecules*., 25(16): 3748.

Srinivasan, K. 2018. Cumin (*Cuminum cyminum*) and black cumin (*Nigella sativa*) seeds: traditional uses, chemical constituents, and nutraceutical effects. *Food Quality Saf*., 2(1): 1-16.

Strothmann, A.L., M.E.A. Berne, G.A. Capella, M.Q. de Moura, T.W. da Silva, C.M. da Costa and N.B. Pinheiro. 2022. Antiparasitic treatment using herbs and spices: A review of the literature of the phytotherapy. *Braz. J. Vet. Med*., 44: e004722.

Younis, A.M., M. Yosri, K. Jennifer and J.K. Stewart. 2019. *In vitro* evaluation of pleiotropic properties of wild mushroom *Laetiporus sulphureus*. *Ann. Agri. Sci*., 64(1): 79-87.

Yusoff, I.M., T.Z. Mat, Z. Rahmat and L.S. Chua. 2022. A review of ultrasound-assisted extraction for plant bioactive compounds: phenolics, flavonoids, thymols, saponins and proteins. *Food Res. Int*., 157: 111268.

Zhang, J., C. Li, M.M. Rahaman, Y. Yao, P. Ma, J. Zhang, X. Zhao, T. Jiang and M. Grzegorzek. 2022. A comprehensive review of image analysis methods for microorganism counting: from classical image processing to deep learning approaches. *Artif. Intell. Rev*., 55(4): 2875-2944.

Zhang, Y., T. Huang, D.M. Jorgens, A. Nickerson, L.J. Lin, J. Pelz, J.W. Gray, C.S. López and X. Nan. 2017. Quantitating morphological changes in biological samples during scanning electron microscopy sample preparation with correlative super-resolution microscopy. *PLoS One*., 12(5): e0176839.